PARAMETRIC SONOGRAPHIC IMAGING – APPLICATION OF SYNTHETIC APERTURE TECHNIQUE TO IMAGING ATTENUATION OF ULTRASOUND IN TISSUE STRUCTURES

JERZY LITNIEWSKI, ZIEMOWIT KLIMONDA, ANDRZEJ NOWICKI

Institute of Fundamental Technological Research, Department of Ultrasound
ul. Pawińskiego 5b, 02-106 Warsaw, Poland
jlitn@ippt.gov.pl

Ultrasonic imaging is a well-established technique in medicine. However, in most conventional applications of clinical ultrasonic scanners only the peak amplitude echogenicity is used to create the image. Moreover, signal envelope detection destroys potentially useful information about frequency dependence of acoustic properties of tissue comprised in RF backscattered echoes. We have explored the possibility of developing the method of imaging the distribution of the acoustic attenuation in tissue. We expect that the method will help in localization of the pathological states of tissue including tumors and diffuse liver diseases. The spatial resolution and precision of the method are crucial for medical diagnosis, hence the synthetic aperture technique was applied for ultrasonic data collection. The final goal of the presented project is to develop reliable diagnostic tool, which could be implemented in standard USG systems, as the new visualization mode.

INTRODUCTION

The ultrasonic imaging (USG) is a non-invasive, popular and relatively inexpensive method of the human body visualization. The USG image consists of many lines; each of them corresponds to the echo envelope. This image reflects the distribution of the tissue reflectivity, that depends on acoustical impedance distribution. However, the raw radio-frequency (RF) echoes contain information about the tissue properties that cannot be assessed with the signal envelope. For example, the frequency dependent attenuation coefficient is an interesting acoustic parameter for tissue characterization with potentially substantial importance in medical diagnostics. Investigations performed in vitro and in vivo showed the correlation between pathological changes in the tissue and variation of the attenuation coefficient. Oosterveld have shown that the slope of attenuation coefficient can be used to diagnose the diffuse liver disease [1]. Saijo and Sasaki employed scanning acoustic microscope to measure five types of gastric cancer and indicated different attenuation

coefficients comparing to the normal tissue [2]. McFarlin et al. investigated possibility of prediction of the premature delivery based on the noninvasive ultrasonic attenuation determination [3]. Pathological processes can lead to changes in the mean attenuation coefficient that range from several percent for cirrhotic human liver, through dozens percent for fatty human liver [4], or degenerated bovine articular cartilage [5] to over a hundred percent in case of porcine liver HIFU treatment in vivo [6] or even more for porcine kidney thermal coagulation [7]. These reports motivated us to consider the parametric imaging of the attenuation as a useful tool in medical diagnostic.

Usually, tissue-attenuating properties averaged over large areas are presented. However, it has been shown that imaging is the best medical diagnostic technique. Conventional ultrasonic imaging as well as other medical visualization methods are successfully applied in all medical fields. Thus, it could be anticipated that also parametric attenuation imaging is a promising diagnostic technique. Although the ultrasound attenuation estimation problem is not new, there is lack of reliable method of estimation it with satisfactory resolution and precision. A lot of researchers were working theoretically and experimentally on tissue attenuation but to the best of our knowledge there is only one group of researchers (Bioacoustics Research Laboratory at the University of Illinois at Urbana-Champaign, USA) working on attenuation distribution imaging [8]. As far their activity is focused on premature delivery prediction from variation of ultrasonic attenuation in cervix.

The purpose of this study was to develop the attenuation parametric imaging technique and to apply it for in vivo characterization of tissue. If succeed, the results of the project will enhance ability of ultrasonic techniques to detect small, pathological tissue lesions.

1.   ESTIMATION OF ATTENUATION COEFFICIENT

There are two approaches to the estimation of the ultrasonic attenuation. The spectral difference technique, that is based on a comparison of the power spectrum of backscattered signals before and after the wave propagation through the medium, and the spectral shift method that uses the downshift of the pulse mean frequency caused by the frequency depended attenuation. In our approach the mean frequency (MF) is directly evaluated from the backscatter data by means of the correlation estimator. We assume, that the attenuation in tissue can be described by the following model. The amplitude of the wave propagating in tissue decreases exponentially due to attenuation what can be expressed as

$$A = A_0 \exp(-\alpha x) \tag{1}$$

where A_0 − initial intensity, α - attenuation coefficient and x − wave path length. The attenuation coefficient depends on frequency f and in the soft tissue it has the following form:

$$\alpha(f) = \alpha_1 \left(\frac{f}{f_1} \right)^n \tag{2}$$

where α_1 is the attenuation coefficient at the frequency f_1 (in the literature generally $f_1=1$ MHz) and n for the soft tissue is close to 1 [9]. Thus, the linear dependence between attenuation coefficient in tissue and the wave frequency is often assumed. When a short ultrasonic pulse propagates in homogenous medium the dispersion of the attenuation coefficient results in the shift of the pulse mean frequency (MF).

We have developed a procedure of attenuation determination from the downshift of mean frequency of the interrogating ultrasonic pulse propagating in the medium. The RF data were collected together with the standard B-scan image. To find estimates of the attenuation from ultrasonic echoes we assumed that the attenuation of tissue increases linearly with frequency and that the backscattered signals have the Gaussian shaped spectra (Gaussian pulses). Then, the MF shift (f–f_0) is given by [10, 11].

$$f - f_0 = \frac{\alpha \cdot \Delta x \cdot \sigma_0^2}{2} \qquad (3)$$

where f_0 and f are MF before and after the wave traveled distance Δx respectively, σ_0^2 is the Gaussian variance of the pulse spectrum and α denotes the attenuation coefficient. Gaussian pulse spectrum preserves the shape during propagation in linearly attenuating medium i.e. the σ_0^2 is constant, and the attenuation coefficient can be calculated from the equation (3).

$$\alpha = -\frac{2}{\sigma_0^2} \frac{\partial f}{\partial x} \qquad (4)$$

The attenuation coefficient is positive, thus MF along the propagation path i.e. the MF line always decreases monotonically with the penetration depth. To determine the MF line we have applied the MF correlation estimator (I/Q algorithm). The estimator is defined by

$$MF = \frac{1}{2\pi T_s} a\tan\left(\frac{\sum_{i=1}^{N} Q(i)I(i+1) - Q(i+1)I(i)}{\sum_{i=1}^{N} I(i)I(i+1) + Q(i+1)Q(i)} \right) \qquad (5)$$

where T_s is the sampling period and N is the estimator window length. The Q and I are quadrature and in-phase signal components. The N is parameter of significant importance because it is directly related to the resolution of the method. The Q and I are obtained by quadrature sampling technique. The quadrature sampling is often used in modern scanners and the correlation estimator is widely used in Doppler techniques [12]. The presented technique of attenuation estimation consists of four steps. First, the raw RF data are filtered with the filter that has bandwidth corresponding to the bandwidth of the transducer. Next, the estimator window moves along the filtered RF line and the MF values are determined. The MF line is created point by point. In ideal case, the attenuation (A) line could be enumerated directly from MF line using the eq. (4). Unfortunately, the real MF lines are highly variable due to the random character of the backscattered RF signals [13, 14] and the direct use of eq. (4) results in the highly noised attenuation values, not acceptable for the attenuation imaging. Thus, in the third step the reduction of the MF line random variability is required. This is realized by the moving average filtration and the Singular Spectrum Analysis (SSA) technique. The moving average filter operating over adjacent MF lines in lateral direction is applied. Then the SSA trend extraction algorithm is employed. In the last step the eq. 4 is applied and the attenuation lines are enumerated from the smoothed MF lines. The SSA is relatively new technique of analysis of the time series. The aim of this technique is the

decomposition of the input data series into the sum of components which can be interpret as the trend, oscillatory components and the noise (non-oscillatory components). The major applications of the SSA technique is the smoothing of the time series, finding the trend, forecasting and detection of the structural changes [15-21]. The SSA is the model-free technique - there is no need to know a general function describing how the MF changes with the depth. Another useful feature of the SSA is its robustness to the outliers [22]. The SSA is easy to use – it needs only one parameter – the window length. Details of this technique can be found in the literature [23]. The application of the SSA and the averaging of the scan lines limits the variations of the attenuation estimate but it is still affected by errors.

2.   ATTENUATION DISTRIBUTIONS DETERMINED IN VIVO WITH CLASSICAL SONOGRAPHY

Two types of ultrasonic data were considered, the B-scan RF images of the skin recorded with the skin scanner operating at 30MHz frequency and the RF images of the liver obtained with Siemens-Antares scanner (5MHz) equipped with Ultrasound Research Interface (URI). The URI enabled direct access to RF echoes.

In Fig.1 the B-scan image of the skin recorded at the nape of the neck together with the equivalent attenuation distribution image is presented. Because the skin can be regarded as the layered structure the time window used for the MF determination was set to 0.5mm and averaging over 60 scans was applied. The attenuation distribution images calculated from the skin B-scans show two oblong areas highly differing in attenuation coefficient value. Significant decrease of attenuation begins approximately 2mm from the skin surface. A difference can be also seen on the B-scan image. The sudden jump in reflectivity at the depth of 2mm corresponds to dermis and hypodermis interface. The mean attenuation coefficient calculated for these two distinct parts of the image along with the standard deviation was equaled to 1.865 ± 0.23 dB/cm·MHz and 0.77 ± 0.69 dB/cm·MHz for dermis-area and hypodermis-area respectively what corresponds well with the published data. The high value of attenuation standard variation in this innermost and thickest layer of the skin reflects complicated structure of hypodermis that consists primarily of loose connective tissue and lobules of fat.

The image of the liver was obtained in vivo together with RF-image and is presented together with the calculated attenuation coefficient distribution (Fig.2). The attenuation coefficient values are much higher for the areas corresponding to the liver tissue comparing to the areas outside of the liver. The coefficient averaged over the liver tissue was equal to 0.59 ± 0.27 dB/cm·MHz what also corresponds well with published data. An increase of the attenuation coefficient at the maximal depth (Fig.2) was probably caused by the noise that limits the depth of attenuation determination to approximately 12 cm. Some variation of attenuation within the liver tissue could be of natural reasons as well as could be caused by not satisfactory focusing compensation. Very high attenuation shown at the liver left border could be caused by reflections at the interface.
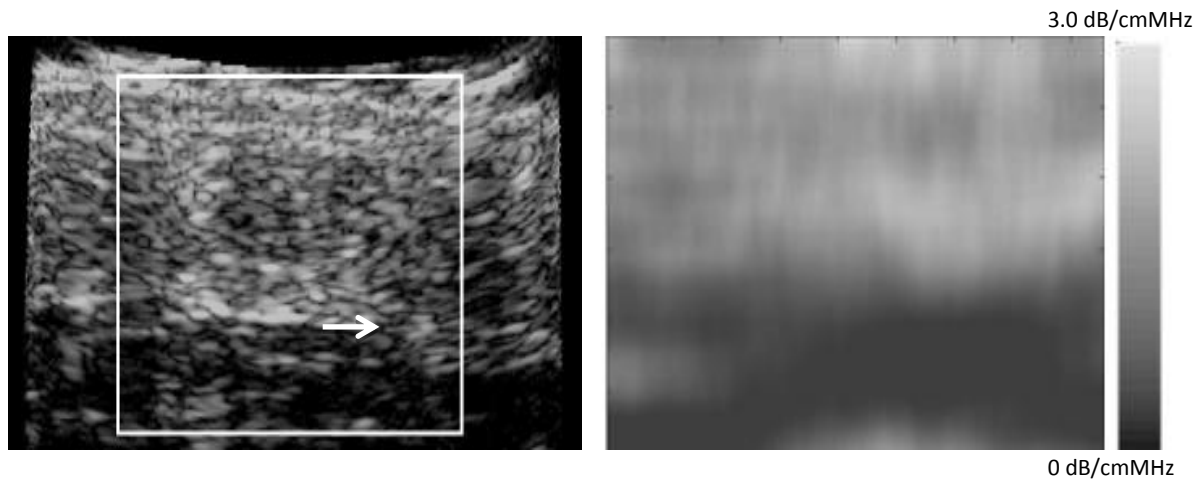
3.0 dB/cmMHz

0 dB/cmMHz

Fig 1. B-scan image (left) and calculated attenuation coefficient distribution (right) obtained in vivo for the skin of the neck. The rectangle marked on the B-scan shows the area where the attenuation was calculated. An arrow shows an approximate location of the interface between dermis and hypodermis.
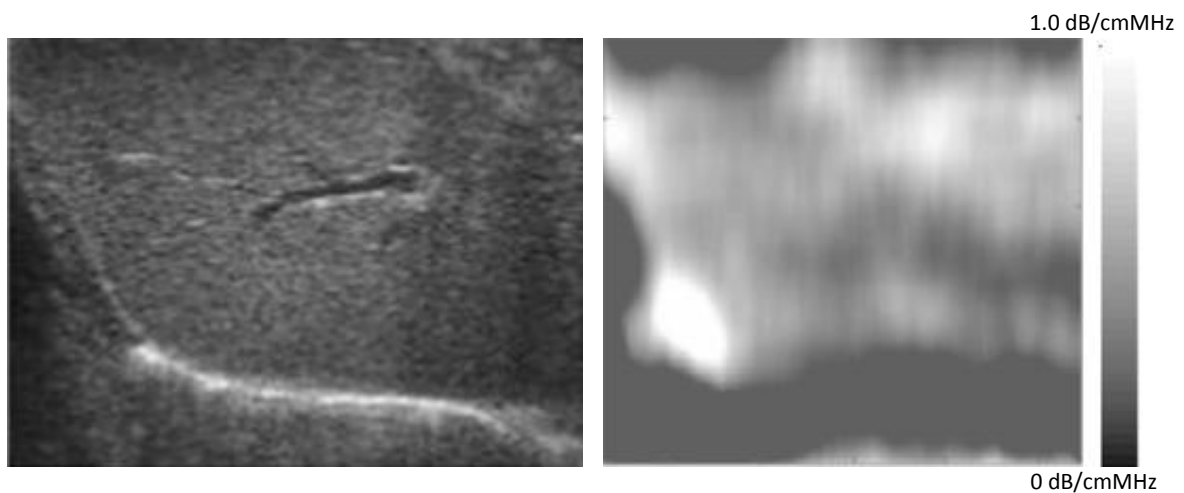
1.0 dB/cmMHz

0 dB/cmMHz

Fig 2. B-scan image (left) and calculated attenuation coefficient distribution (right) obtained in vivo for the liver.

While the averaged values of attenuation coefficient are in good agreement with published data the spatial resolution of attenuation imaging is poor. The higher spatial resolution is required to create an ultrasound attenuation imaging system which can quantitatively measure the attenuation coefficient in tissues and accurately discriminate tissue degeneration areas from normal areas in early stages by imaging attenuation distribution. Attenuation is estimated from the stochastic ultrasonic backscatter and averaging is necessary to achieve reasonable accuracy. However averaging worsen the spatial resolution. Synthetic

Aperture Focusing (SAF) technique gives very good results in standard ultrasonography, considerably increasing the image resolution. We hope that application of this technique to acquire the ultrasonic data that are letter processed to extract the tissue attenuation, will increase the quality (resolution and accuracy) of attenuation images.

3. THE SYNTHETIC APERTURE TECHNIQUE

The idea of Synthetic Aperture (SA) in radar technique reaches the early fifties. Fast progress in electronic and signal processing made possible to build the first SA radar in about 1970 [24]. Since then the rapid growth of this method is observed in a wide field of applications. From earth observing satellites, airborne radars to hydroacoustic issues, like sonars. Recently, it is used in ultrasonic imaging. The main idea behind Synthetic Aperture method is to reconstruct image lines not only on base of single RF acquisition for that line (on Real Aperture). The conception is to gather signals emitted from successive points in space, which position is exactly known and to reconstruct the image on base of all emissions. The bigger (Synthetic) aperture is then created and reconstructed images have higher quality (resolution) then images achieved in classical way. More details on Synthetic Aperture can be found in [25-27]. One of the most important feature of SA method according to ultrasonic imaging is the fact that it is a coherent imaging method. In this technique we are focusing on every single point by proper correction of RF data phases when reconstructing the image. That makes this method very attractive for medical data visualization due to good resolution in the full depth of scanned area. In classical beamforming method we obtain the best resolution in the focus of ultrasound beam and its nearest neighborhood. It makes that the final images have areas with different resolution quality. This effect can be reduced by increasing the number of focus points. However a high number of transmissions required in that approach can significantly reduce the frame rate - an important parameter in medical imaging. Hence, the usage of SA technique appears to be an optimal solution.

The idea of using SA technique for acquiring RF data that are next processed for attenuation determination is twofold. We know that focusing introduce variation of pulse spectrum what results in incorrect assessment of attenuation. This effect of focusing must be compensated. For standard delay and sum beam forming (DAS) the focusing is performed only in several, fixed distances in the tissue. Thus the influence of focusing varies along the echo line. In case of SA technique the focusing is performed (in practice) in all points of imaging tissue and its influence on the signal spectrum is very similar in the whole imaging area. Thus the correction of focusing effects is much easier and more effective in case of SA. Also, the attenuation imaging requires application of averaging over adjacent echo lines and along the line. That reduces the spatial resolution of attenuation images. In a case of SA the averaging is much more effective because the areas in the vicinity of focus are statistically independent and only averaging over few of them is necessary to reduce stochastic factors in calculated attenuation. Out of focus (the case for the most of the imaging area when the standard beam forming is used) the areas insonificated by adjacent beams are overlapping and more averaging is required what worsen the resolution of attenuation map. Some basic transmit/receive schemes of SA in ultrasonic imaging are presented below:
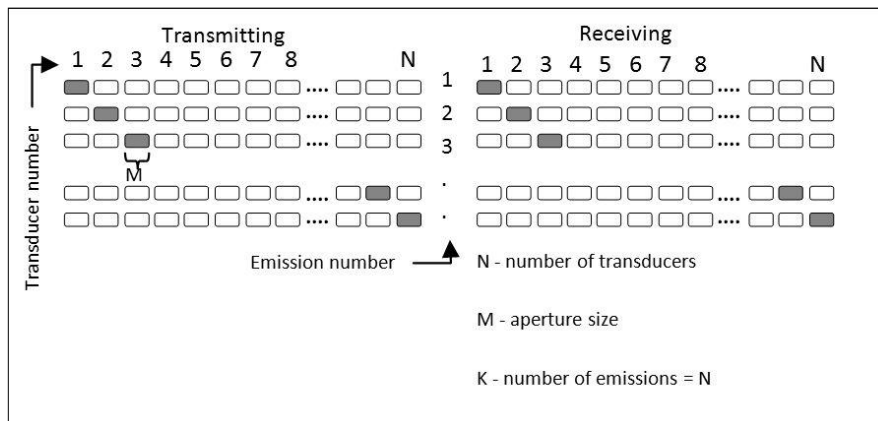
Synthetic Aperture Focusing (SAF)

Fig.3 Scheme of SAF mode.

Figure 3 describes the emission scheme of Synthetic Aperture Focusing (SAF).This is the simplest version of SA method due to usage of one channel only. In each step echoes are transmitted and received with a single element of linear array. In each step the next element is activated until the RF data from all channels is being collected. The main disadvantage of this scheme is a small signal power, that can be transmitted using single element. The Signal-to-Noise ratio (SNR) is in this case on the lowest level. Hence, the maximal penetration depth is insufficient for typical diagnosing purposes.

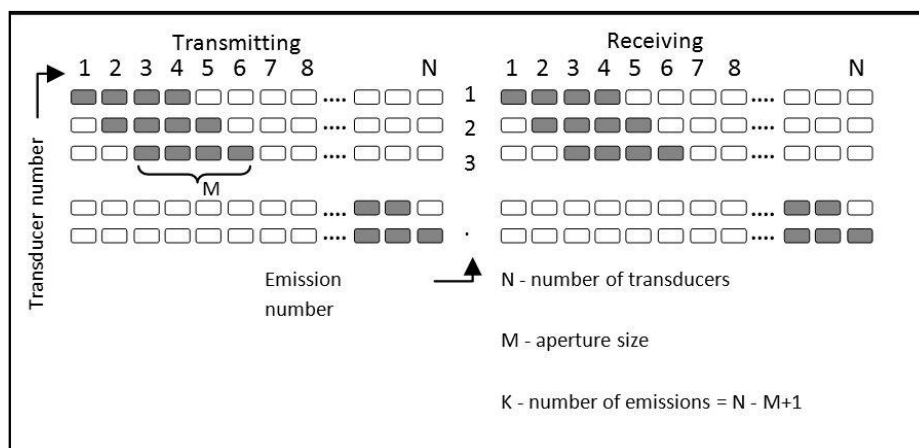Multi-element Synthetic Aperture Focusing (M-SAF)

Fig.4 Scheme of M-SAF mode.

Figure 4 shows the principles of Multi-element Synthetic Aperture Focusing. The significant difference in comparison to previous scheme is that the group of transducers is used instead of a single element. This method provides higher emission power (better SNR), because a higher number of transducers is used.
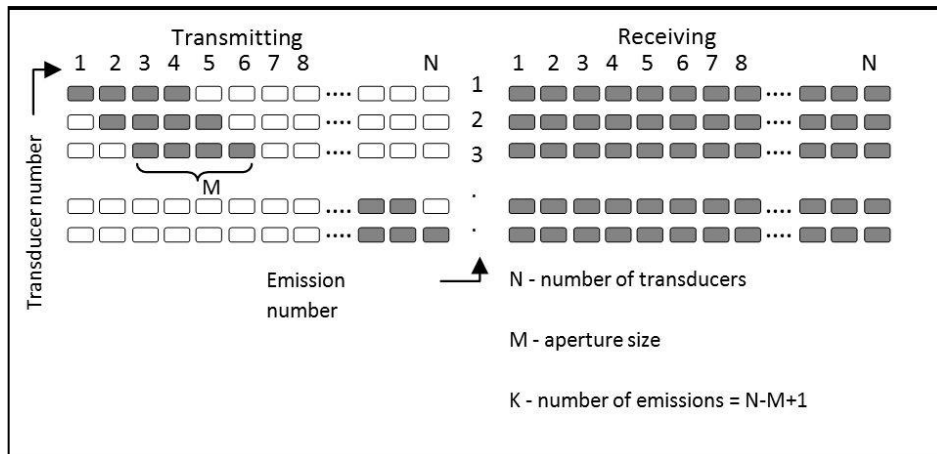
Synthetic Transmit Aperture (STA)

Fig.5 Scheme of STA mode.

Synthetic Transmit Aperture (STA) is a modification of M-SAF technique and is described in figure 5. In this method the full receive aperture is used for all steps, which positively influences reconstructed images, because larger receiving aperture provides higher SNR and better lateral resolution.

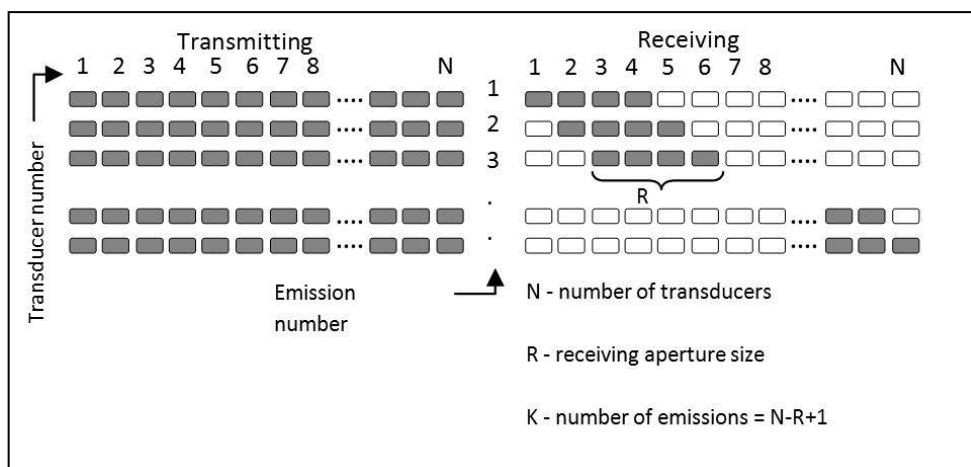Synthetic Receive Aperture (SRA)

Fig.6 Scheme of SRA mode.

Synthetic Receiving Aperture (SRA) scheme is presented in figure 6. In this case all transmissions are performed with use of full aperture. The receiving sequences are divided into sub-apertures. This solution enables reducing of the number of active receiving channels.

4.   RESULTS

The experimental data were recorded using ultrasonic scanner (UltrasonixSonic TOUCH) equipped with linear probe (126 elements) and operating at 7.0 MHz frequency. The system enables a full control of the transmission and reception giving access to every single piezo-element of multi-elements ultrasonic probe. The RF data were collected applying SAF scheme with one element transmitting and all elements receipting. Next the data were processed and attenuation map was created. The resolution and accuracy of the method was verified using tissue mimicking phantom with uniform echogenicity but varying attenuation coefficient. The phantom consists of two cylinders of 1.5 cm diameter with attenuation coefficient equal to 0.9 and 0.7 dB/(MHz·cm), respectively that were embedded in the medium with attenuation of 0.5 dB/(MHz·cm) at the depth of 3 cm.

The images obtained by using SA technique and SonicTOUCH system are presented in Fig.7 and Fig.8. The objects are invisible in B-mode and clearly visible in attenuation images.
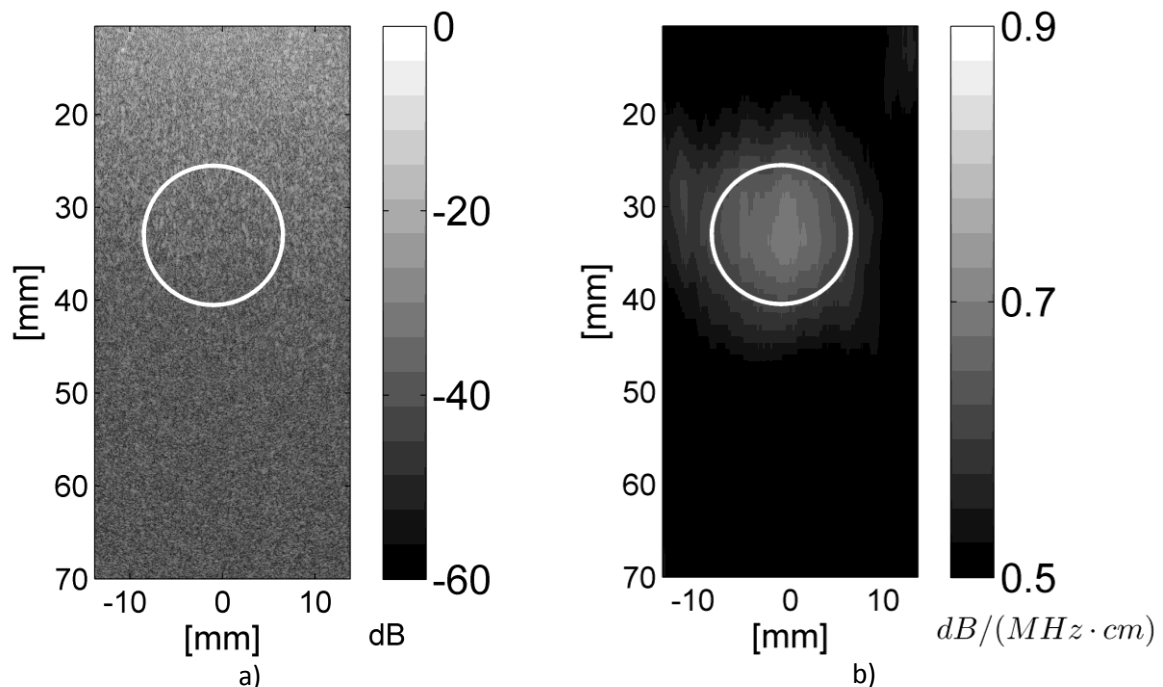

Fig. 7. The standard B mode image (a) and the attenuation map (b) present the attenuating object in tissue mimicking phantom. The attenuation of background and the object was equal 0.5 and 0.7 dB/(MHz·cm) respectively.
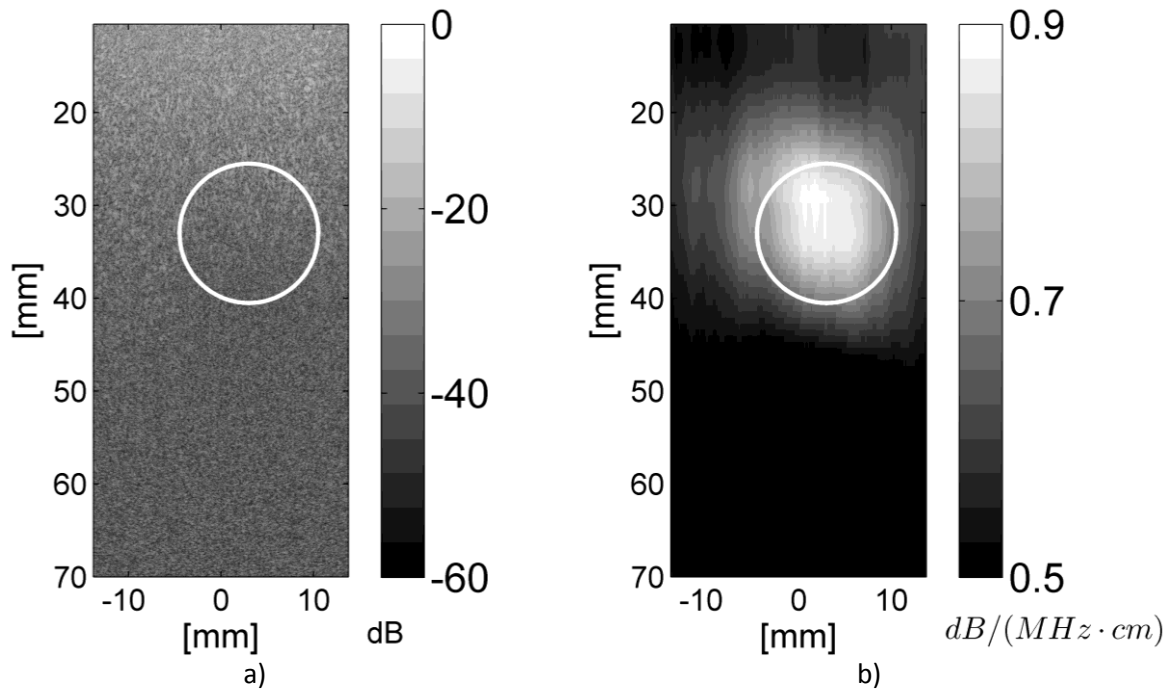
Fig. 8. The standard B mode image (a) and the attenuation map (b) present the attenuating object in tissue mimicking phantom. The attenuation of background and the object was equal to 0.5 and 0.9 dB/(MHz·cm) respectively.

5. CONCLUSIONS

Mean frequency correlation estimator and SSA technique were implemented for processing of the RF ultrasonic echoes. The estimated attenuation values were equal to 0.7 and 0.9 dB/(MHz·cm) and agreed well with the real values. We have found that the RF data obtained using synthetic aperture focusing technique (SAF) were much more reliable considering attenuation extraction then the echoes recorded applying standard delay and sum beamforming. The imaging of attenuation in tissue seems to be promising technique in medical diagnostics, however the precision of a single scan is often unsatisfactory. The synthetic transmit aperture technique allows to obtain the similar quality images as spatial compounding technique that utilize a dozen or so images for averaging. The SAF technique uses a single scan only, what is more suitable for the real time application. The presented technique allows to visualize the variation of attenuation coefficient as low as 0.1 dB/(MHz·cm) with the spatial resolution of 15 mm.

REFERENCES

[1]   B. J. Oosterveld, J. M. Thijssen, P. C. Hartman, R. L. Romijn, and G. J. Rosenbusch, Ultrasound attenuation and texture analysis of diffuse liver disease: methods and preliminary results. Phys. Med. Biol., 36(8), 1039-1064, 1991

[2]   Y. Saijo and H. Sasaki, High frequency acoustic properties of tumor tissue. In F. Dunn, M. Tanaka, S. Ohtsuki, and Y Saijo., editors, Ultrasonic Tissue Characterization, chapter 12, pages 217–229. Springer-Verlag, Tokyo, 1996.

[3] B. L. Mcfarlin, T. A. Bigelow, Y. Laybed, W. D. O'brien, M. L. Oelze, J. S. Abramowicz, Ultrasonic attenuation estimation of the pregnant cervix: a preliminary results, Ultrasound in Obstetrics and Gynecology, 36, 218-225, 2010.

[4] Z. F. Lu, J. Zagzebski, and F. T. Lee, Ultrasound backscatter and attenuation in human liver with diffuse disease. Ultrasound Med. Biol., 25(7), 1047-1054, 1999.

[5] H. J. Nieminen, S. Saarakkala, M. S. Laasanen, J. Hirvonen, J. S. Jurvelin, and J. Töyräs, Ultrasound attenuation in normal and spontaneously degenerated articular cartilage, Ultrasound Med. Biol., 30(4), 493-500, 2004.

[6] V. Zderic, A. Keshavarzi, A. M. Anrew, S. Vaezy, and R. W. Martin, Attenuation of porcine tissues in vivo after high intensity ultrasound treatment, Ultrasound Med. Biol., 30(1), 61-66, 2004.

[7] A. E. Worthington and M. D. Sherar, Changes in ultrasound properties of porcine kidney tissue during heating, Ultrasound Med. Biol., 27(5), 673-682, 2001.

[8] Y. Labyed, T. A. Bigelow, B. L. McFarlin, Estimate of the Attenuation Coefficient Using a Clinical Array Transducer for the Detection of Cervial Ripening in Human Pregnancy, Ultrasonics, 51, 34-39, 2011.

[9] A. Nowicki, Ultrasonic Diagnostics [in Polish], MAKmed, Gdańsk2000.

[10] P. Laugier, G. Berger, M. Fink, , J. Perrin, Specular reflector noise: effect and correction for in vivo attenuation estimation, Ultrasonic Imaging 7, 277-292, 1985.

[11] J. Litniewski, Assessment of trabecular bone structure deterioration by ultrasound [in Polish], Prace IPPT,2006.

[12] A. Nowicki, Fundamentals of Doppler Ultrasonography [in Polish], PWN 1995.

[13] Z. Klimonda, , A. Nowicki, Imaging of the mean frequency of the ultrasonic echoes, Archives of Acoustics, 32(4) (supplement), 77-80, 2007.

[14] J. Ophir, M. A. Ghouse, L. A. Ferrari, Attenuation estimation with the zero crossing technique: phantom studies, Ultrasonic Imaging, 7, 122-132, 1985.

[15] F. J. Alonso, J. M. Del Castillo, P. Pintado, Application of singular spectrum analysis to the smoothing of raw kinematic signals, Journal of Biomechanics, 38, 1085-1092, 2005.

[16] N. E. Golyandina, K. D. Usevich, I. V. Florinsky, Filtering of Digital Terrain Models by Two-Dimensional Singular Spectrum Analysis, International, Journal of Ecology & Development, 8(f07), 81-94, 2007.

[17] H. Hassani, Singular Spectrum Analysis: Methodology and Comparison, Journal of Data Science, 5, 239-257, 2007.

[18] J. C. Moore, A. Grinsted, Signular spectrum analysis and envelope detection: methods of enhancing the utility of ground-penetrating radar data, Journal of Glaciology, 52(176) 159-163, 2006.

[19] D. H. Schoellhamer, Singular spectrum analysis for time series with missing data, Geophysical Research Letters, 28(16), 3187-3190, 2001.

[20] F. Varadi, R. K.Ulrich, L. Bertello, C. J. Henney, Random lag singular cross-spectrum analysis, The Astrophysical Journal, 528(1), L53-L56, 2000.

[21] R. Vautard, P. Yiou, M. Ghil, Singular-spectrum analysis: a toolkit for short, noisy chaotic signals, Physica D, 58, 95-126,1992.

[22] T. Alexandrov, A Method of Trend Extraction using Singular Spectrum Analysis, REVSTAT Statistical Journal, 7(1), 1-22,2009.

[23] N. Golyandina, V. Nekrutkin, A. Ahigljavsky, Analysis of time Series Structure: SSA and related techniques, Chapman & Hall/CRC, 2001.

[24] R. Bamler, Principles of Synthetic Aperture radar, Surveys in Geophysics 21, 147-157,2000.

[25] J. A. Jensen, S.I. Nikolov, K.L. Gammelmark, M.H. Pedersen, Synthetic aperture ultrasound imaging, Ultrasonics 44,e5–e15, 2006.

[26] C. A. Willey, Synthetic aperture radars – a paradigm for technology evolution. IEEE Trans. Aerospace Elec. Sys., 21, 440-443, 1985.

[27] J. C. Curlander, R. N. McDonough, Synthetic aperture radar systems and signal processing. John Wiley&Sons, New York.

[28] I. Malecki, Theory of acoustic waves and systems [in Polish], 1964.

[29] P. A. Magnin, O. T. von Ramm, F. L. Thurstone, Frequency compounding forspeckle contrast reduction in phased array images, Ultrasonic Imag. 4, 267-281, 1982.

[30] M. Sęklewski, P. Karwat, Z. Klimonda, M. Lewandowski, A. Nowicki, Preeliminary results: comparison of different schemes of synthetic aperture technique in ultrasonic imaging, Hydroacoustics, 6, 243-252, 2010.

[31] P. Karwat, Z. Klimonda, M. Sęklewski, M. Lewandowski, A. Nowicki, Data Reduction Method for Synthetic Transmit Aperture Algorithm. Archives of Acoustics, 9, 635-642, 2010.

[32] A. Nowicki, Z. Klimonda, M. Lewandowski, J. Litniewski, P. A. Lewin, I Trots, Comparison of sound fields generated by different coded excitations--experimental results, Ultrasonics, 44(1), 121-129, 2006.

[33] J. Litniewski, A. Nowicki, Z. Klimonda, M. Lewandowski, Sound Fields for Coded Excitations in Water and Tissue: Experimental Approach, Ultrasound in Medicine & Biology, 33(4), 601-607, 2007.